iScience

CellPress
OPEN ACCESS

Article

Protection from acute lung injury by a peptide designed to inhibit the voltage-gated proton channel

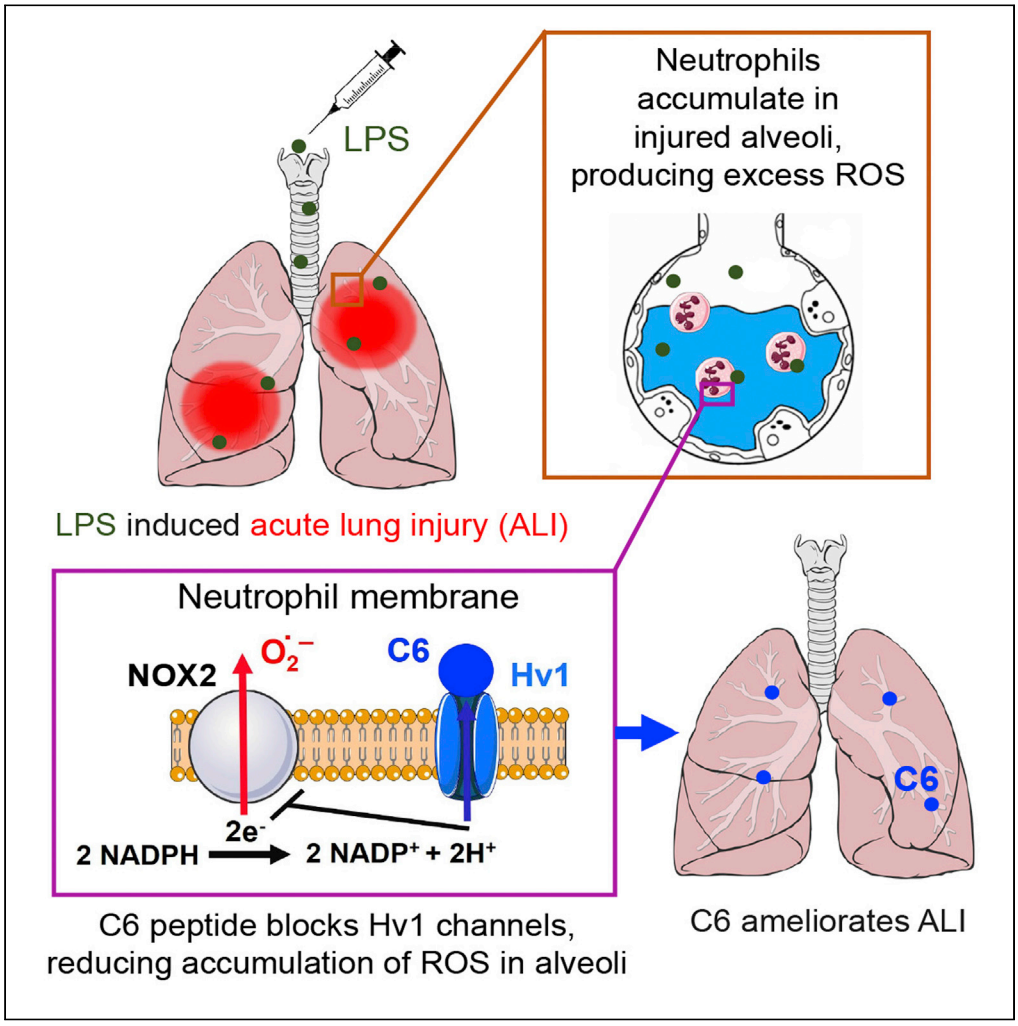

Ruiming Zhao, Benjamin Lopez, Andreas Schwingshackl, Steve A.N. Goldstein

aschwingshackl@mednet.ucla.edu (A.S.)
sgoldst2@uci.edu (S.A.N.G.)

Highlights

C6 suppresses Acute Lung Injury (ALI) induced in mice by intratracheal bacterial LPS

C6 inhibits Hv1 channels to reduce neutrophil influx and inflammatory mediator release

Genetic knockout experiments in mice confirm the *in vivo* target for C6 is Hv1

Inhibition of Hv1 by C6 is a targeted therapeutic approach for LPS-induced ALI

Zhao et al., iScience *26*, 105901
January 20, 2023
https://doi.org/10.1016/j.isci.2022.105901

iScience

CellPress
OPEN ACCESS

Article

Protection from acute lung injury by a peptide designed to inhibit the voltage-gated proton channel

Ruiming Zhao,[1] Benjamin Lopez,[2] Andreas Schwingshackl,[2,*] and Steve A.N. Goldstein[1,3,*]

SUMMARY

There are no targeted medical therapies for Acute Lung Injury (ALI) or its most severe form acute respiratory distress syndrome (ARDS). Infections are the most common cause of ALI/ARDS and these disorders present clinically with alveolar inflammation and barrier dysfunction due to the influx of neutrophils and inflammatory mediator secretion. We designed the C6 peptide to inhibit voltage-gated proton channels (Hv1) and demonstrated that it suppressed the release of reactive oxygen species (ROS) and proteases from neutrophils *in vitro*. We now show that intravenous C6 counteracts bacterial lipopolysaccharide (LPS)-induced ALI in mice, and suppresses the accumulation of neutrophils, ROS, and proinflammatory cytokines in bronchoalveolar lavage fluid. Confirming the salutary effects of C6 are via Hv1, genetic deletion of the channel similarly protects mice from LPS-induced ALI. This report reveals that Hv1 is a key regulator of ALI, that Hv1 is a druggable target, and that C6 is a viable agent to treat ALI/ARDS.

INTRODUCTION

Acute lung injury (ALI) and its most severe form Acute Respiratory Distress Syndrome (ARDS) are common, life-threatening sequelae in patients with bacterial pneumonia or SARS-CoV-2 infection.[1,2] ALI/ARDS is defined as a non-cardiogenic lung disease with acute onset characterized by diffuse bilateral pulmonary infiltrates due to alveolar inflammation and alveolar-capillary barrier dysfunction resulting in lung edema with protein-rich fluid that impairs arterial oxygenation. ALI/ARDS is seen in ~190,000 patients in the United States each year in the association of ~74,500 deaths.[3] After five decades of effort, there are no disease-modifying drugs for ALI/ARDS and management remains supportive, in-part because many downstream processes are dysregulated as the disease progress leading to complex pathophysiology and patient heterogeneity.[1,2]

Neutrophils are the most abundant human phagocytes, accounting for 50-60% of circulating white blood cells, and are usually the first cells to arrive at sites of infection.[4] Accumulation of neutrophils in the lungs is recognized as one of the hallmark features of ALI/ARDS.[5] Neutrophils are recruited to the lung by inflammatory chemokines[4] where they release reactive oxygen species (ROS), proteases and cytokines, all of which play a role in killing pathogens but are also injurious because they damage the alveolar-capillary barrier allowing protein-rich fluid to accumulate in the alveoli, impeding gas exchange.[6] Indeed, in patients with ALI/ARDS the degree of ROS elevation in bronchioalveolar lavage (BAL) fluid and the extent of neutrophilia correlate with disease severity and mortality rates, respectively.[5,6]

The human voltage-gated proton channel (hHv1) is a H^+-selective channel that opens and closes in response to changes in the transmembrane potential and pH gradient.[7] The channel is expressed in neutrophils where it mediates acid extrusion and membrane potential compensation required for the innate immune response.[8–10] C6 is a peptide we created to block hHv1 with high specificity and affinity.[8] We isolated C6 by designing ~1 million unique peptides based on the sequences of 110 natural venom toxins, expressing the peptides on phage, and selection of peptides based on high-affinity phage binding to immobilized, purified hHv1 protein.[8] C6 inhibits hHv1 with an equilibrium affinity of 1.5 nM at 0 mV, binding with positive cooperativity to the two voltage sensors in the channel and holding them in the down conformation that favors channel closure (Figure S1A).[8,11]

Prior to our design of C6, all known hHv1 inhibitors were pharmacologically promiscuous or of low affinity.[7] With C6, we were able to show that proton efflux via hHv1 is required in human sperm to allow the acrosomal

[1]Departments of Pediatrics, Physiology & Biophysics, and Pharmaceutical Sciences, Susan and Henry Samueli College of Health Sciences, University of California, Irvine, Irvine, CA 92697, USA

[2]Department of Pediatrics, University of California, Los Angeles, Los Angeles, CA 90095, USA

[3]Lead contact

*Correspondence: aschwingshackl@mednet.ucla.edu (A.S.), sgoldst2@uci.edu (S.A.N.G.)

https://doi.org/10.1016/j.isci.2022.105901

reaction and oocyte fertilization and in isolated human neutrophils to allow sustained release of ROS and proteases.[8,12] Demonstrating the latter function *in vitro* supported the hypothesis that Hv1 in neutrophils was important in an array of inflammatory disorders,[13] and led us to pursue this *in vivo* study. Based on the correlation of pulmonary neutrophilia and ALI/ARDS severity, we posited that the C6 blockade of Hv1 would inhibit the neutrophil inflammatory response and suppress inflammatory lung injury. To test this proposition, we administered C6 intravenously (*i.v.*) in a well-characterized mouse model for ALI induced by intratracheal (*i.t.*) bacterial lipopolysaccharide (LPS),[14] and confirmed the specificity of C6 for Hv1 *in vivo* using Hv1-deficient mice. Both pharmacological inhibitions of Hv1 with C6 and Hv1 deletion protected mice from LPS-induced ALI and accumulation of ROS in lungs, validating the therapeutic potential of C6 and Hv1 as a target.

RESULTS

C6 protects pulmonary function and decreases alveolar inflammation in lipopolysaccharide-treated mice

LPS is a major component of the outer membrane of Gram-negative bacteria. In humans, *i.t.* the administration of LPS in healthy volunteers acts as an inflammatory stimulant that leads to neutrophil recruitment to the lungs by chemokines, increased alveolar-capillary permeability, and the accumulation of neutrophils, fluid, and protein in the pulmonary airspaces, that is, hallmarks of infectious ALI.[15] In mice, *i.t.* instillation of LPS produces inflammation and lung injury that recapitulates many of the findings of human ALI, including the migration of neutrophils into the alveolar air spaces, direct alveolar epithelial damage, and pulmonary edema.[14] A schematic representation of our ALI model is shown in Figure 1A. In our hands, *i.t.* administration of LPS (10 mg/kg) to mice produced the characteristic hallmarks of ALI. Histological analyses and blinded lung injury scoring of hematoxylin and eosin (H&E) stained lung sections revealed severe lung tissue damage with interstitial thickening and interstitial neutrophilic infiltration in the LPS-treated mice compared to control animals (Figures 1B and 1C). Decreased lung compliance ($\Delta V/\Delta P$), a measure of the lung expandability that quantifies the change in volume in the lungs (ΔV) caused by transpulmonary pressures (ΔP), is a prominent feature of human ALI and was observed in the LPS-treated mice (Figure 1D). We also observed the sequelae of increased alveolar-capillary permeability in the LPS-treated mice, including the accumulation of protein-rich BAL fluid (Figure 1E).

To mimic a clinically relevant treatment model, two doses of C6 were administered *i.v.* to WT mice 5 and 24 h after *i.t.* LPS administration (Figure 1A) at either 4 mg/kg (C6 low) or 12 mg/kg (C6 high). Histological analysis and blinded lung injury scoring of H&E-stained lung sections revealed that the administration of C6 reduced tissue damage (Figures 1B and 1C). Further, compared to the vehicle control group, C6 significantly improved lung compliance and decreased BAL fluid protein (Figures 1D and 1E). While C6 improved lung compliance in a dose-dependent manner, with the low dose producing a significant improvement that was enhanced by the high dose (Figure 1D), the decrease in the lung injury score (Figure 1C) and BAL protein level achieved by the low C6 dose was not improved upon by the higher dose (Figure 1E).

C6 reduces neutrophil influx and reactive oxygen species levels in the lungs of lipopolysaccharide-treated mice

Neutrophils enter the lungs and release ROS to combat infection, but these responses can also initiate and propagate inflammatory injury.[6] Because we observed improved pulmonary function after the administration of *i.v.* C6 to the LPS-treated mice, we anticipated the peptide might have also reduced neutrophil influx and lowered ROS levels in the lungs; this was the case. Whereas neutrophil counts were negligible in healthy mouse lungs (Figure 2A), *i.t.* LPS administration yielded an influx (Figure 2A) increasing neutrophil counts to ~93% of the total BAL fluid cell count (Figure 2B), a neutrophilic predominance like that observed in patients with bacterial ALI.[5] Consistent with the prior histological analysis (Figure 1B) administration of C6 (C6 low, 4 mg/kg) reduced the neutrophil cell count by 60% (Figure 2A). Further, ROS production by BAL neutrophils in LPS-treated mice was significantly elevated compared to the vehicle control group whereas *i.v.* administration of C6 at 4 mg/kg decreased ROS in the LPS-treated mice by 53% (Figure 2C). Of note, the high dose of C6 (12 mg/kg) did not reduce neutrophil counts and ROS levels in BAL more effectively than the low dose (Figures 2A and 2C).

C6 reduces the levels of proinflammatory cytokines in the lungs of lipopolysaccharide-treated mice

During ALI, hyperactive innate immune cells produce excess proinflammatory cytokines exacerbating pulmonary inflammation.[1,2] For example, elevated levels of Interleukin 6 (IL-6) are a biomarker for poor outcomes in

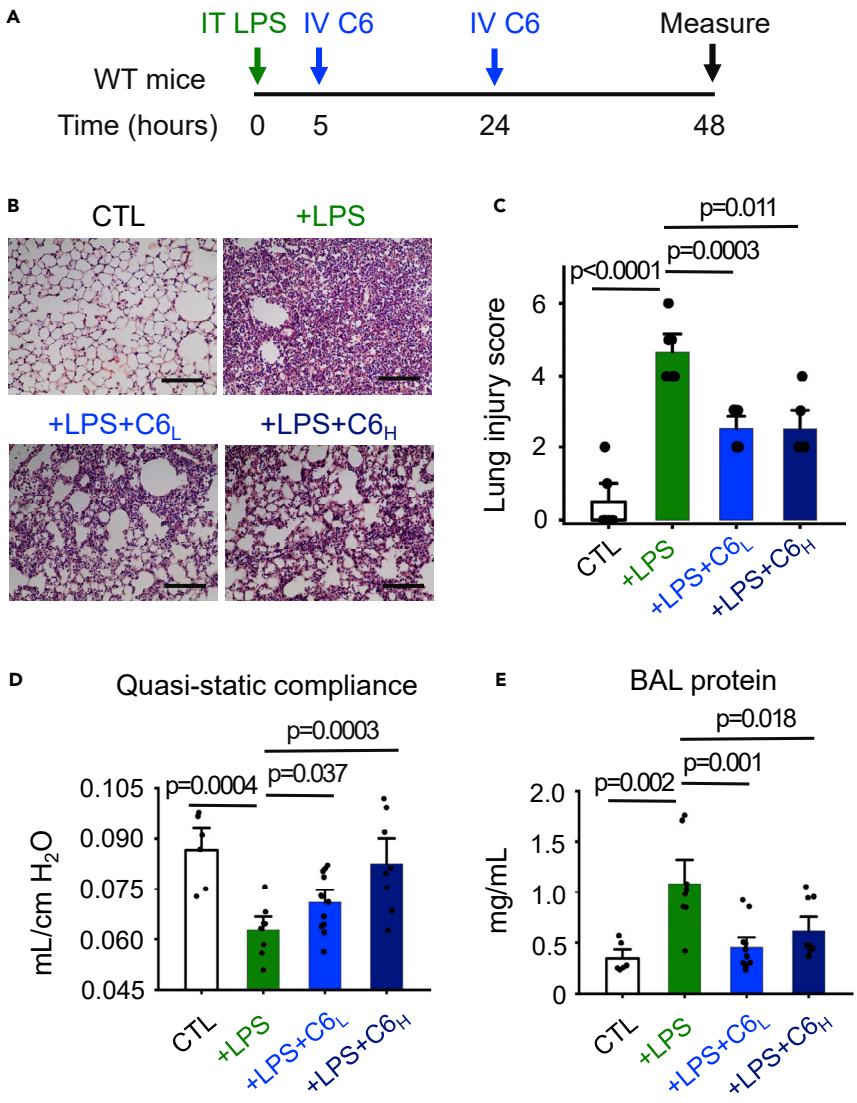

Figure 1. C6 peptide ameliorates LPS-induced ALI.

Experiments were conducted using C57BL/6 WT mice (age- and sex-matched, n = 6-12). C6 was intravenously (*i.v.*) injected via the retro-orbital vein and the pulmonary parameters were measured 48 h post intratracheal (*i.t*) instillation of LPS, as described in STAR Methods. Values are mean ± SEM.

(A) Delayed two-dose C6 *i.v.* administration protocol to mimic a clinically relevant treatment model.

(B) Representative images of H&E-stained lung sections of WT mice exposed to LPS for 48 h with or without C6 treatment (scale bars = 200 μm). Two concentrations of C6, high concentration $C6_H$ = 12 mg/kg and low concentration $C6_L$ = 4 mg/kg were tested. Mice in the C6 group received two doses (*i.v.*) injections of C6 peptide as illustrated in panel A, the control group received injections of PBS, and the LPS group received injections of LPS (10 mg/kg) + vehicle control (DMSO:PBS = 1:20).

(C) Summary of cumulative lung injury scores, which were determined by an investigator blinded to the experimental conditions on H&E-stained lung sections as described in STAR Methods. Two sets of slides were prepared and analyzed for each mouse, and samples from three mice were analyzed for each group (n = 6 slides).

(D) Quasi-static lung compliance measurements for WT mice subjected to LPS-induced ALI without or with either high concentration (12 mg/kg) or low concentration C6 (4 mg/kg) treatment.

(E) Bronchoalveolar lavage (BAL) fluid total protein measurements for WT mice subjected to LPS-induced ALI without or with either high concentration (12 mg/kg) or low concentration C6 (4 mg/kg) treatment.

patients with ALI/ARDS.[2] Therefore, we studied the effect of C6 on the levels of six clinically relevant cytokines in BAL fluid from LPS-treated mice by ELISA. Again, C6 proved effective, suppressing BAL fluid levels of IL-6, chemokine (C-C motif) ligand 2 (CCL2), C-X-C motif chemokine ligand 10 (CXCL10), Interleukin-1β (IL-1β) and

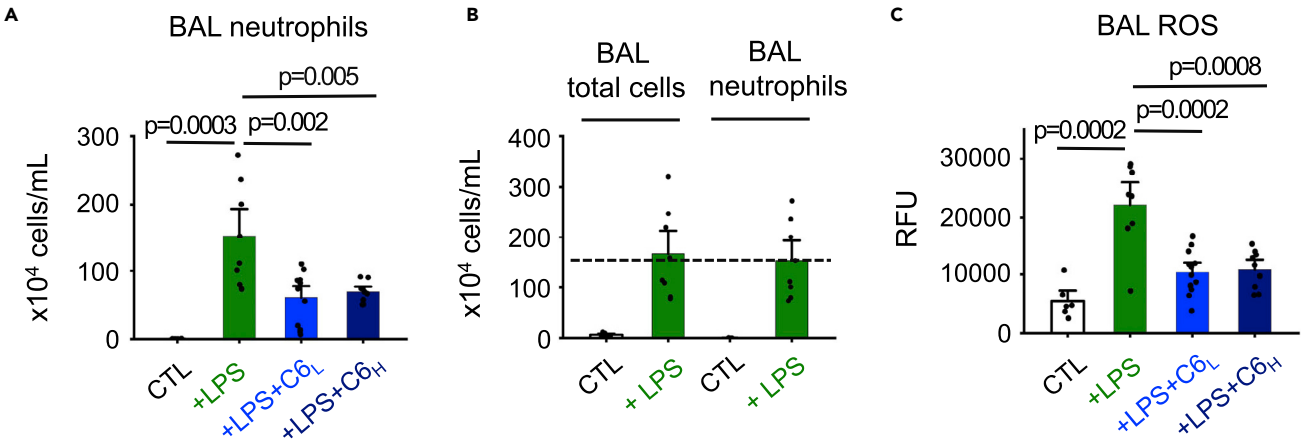

Figure 2. C6 reduces neutrophils and ROS accumulation in LPS-induced mice.

Neutrophil counts and ROS levels in BAL fluids of mice (age- and sex-matched, n = 6-12) were determined as described in the STAR Methods. LPS and C6 were administered as described in Figure 1. Control groups received injections of PBS. Values are mean ± SEM.

(A) BAL neutrophils count for WT mice subjected to LPS-induced ALI without or with either high concentration C6 (12 mg/kg) or low concentration C6 (4 mg/kg) treatment.

(B) *i.t* instillation of LPS increased total cell number in BAL fluid, among which neutrophils accounted for ~93% of cells.

(C) ROS production from BAL neutrophils of WT mice subjected to LPS-induced ALI without or with either high concentration (12 mg/kg) or low concentration C6 (4 mg/kg) treatment using a kit that measures the fluorescence of carboxy-H2DCFDA after intracellular oxidation.

macrophage inflammatory protein-1 alpha (MIP-1α), without significantly changing the level of tumor necrosis factor alpha (TNF-α) (Figure 3).

Genetic deletion of mHv1 also protects mice from lipopolysaccharide-induced ALI

To validate the target of C6 as Hv1, we employed a homozygous Hv1 knockout mouse ($Hv1^{-/-}$) created with genetrap technology that was generously shared.[9,16] $Hv1^{-/-}$ mice lack detectable Hv1 protein in peripheral leukocytes, and ROS production by neutrophils stimulated with phorbol myristate acetate (PMA) is diminished.[9] Here, we treated the $Hv1^{-/-}$ mice with *i.t.* LPS and observed that they were protected compared to WT mice, showing marked preservation of lung compliance (Figure 4A). Further, LPS-induced ROS production was reduced by ~62% in the BAL fluid of $Hv1^{-/-}$ mice (Figure 4B). In contrast, neutrophil predominance and protein levels were elevated like they were in LPS-treated WT mice (Figures 4C and 4D). Whereas C6 inhibited the rise of five cytokines in BAL fluid of LPS-treated mice but not TNF-α (Figure 3), LPS-treated $Hv1^{-/-}$ mice showed only a significant decrease in the level of TNF-α (Figure 5). We also administered LPS to heterozygous mice to study animals with decreased Hv1 ($Hv1^{+/-}$) to investigate if deficiency might mimic WT mice treated with C6 where channel function is inhibited but not absent. Whole-cell patch clamp with neutrophils isolated from WT, $Hv1^{+/-}$ and $Hv1^{-/-}$ mice confirmed that the Hv1 current density in $Hv1^{+/-}$ mice (measured at +80 mV) was ~3-fold smaller than that in WT mice, suggesting a decrease of the expression level of Hv1 of ~70%, and the absence Hv1 current in $Hv1^{-/-}$ mice (Figure S2). As expected, $Hv1^{+/-}$ mice were protected from *i.t.* LPS-induced loss of lung compliance compared to WT mice (Figure 4A) and showed LPS-induced ROS production in BAL fluid that was reduced by ~35% (Figure 4B). Of note, $Hv1^{+/-}$ and $Hv1^{-/-}$ mice showed elevated BAL protein and neutrophil counts in response to LPS like WT mice that did not receive C6 (Figures 4C and 4D).

C6 inhibits mHv1 H^+ currents

We chose to administer 12 mg C6 per kg in mice (C6 high dose) to achieve an initial tissue concentration of ~3,000 nM (STAR Methods) based on *in vivo* peptide toxin distribution studies by others.[17] Since we isolated C6 to inhibit human Hv1,[8] it was important to determine that C6 also effectively blocked mouse Hv1 (mHv1) to validate conclusions drawn from the *in vivo* studies. Consistent with the same voltage sensor-trapping mechanism described for the human channel,[8,11] C6 decreased outward H^+ currents through mHv1 channels expressed in HEK293T cells in response to depolarizing steps measured by whole-cell patch clamp recording (Figure 6A) by shifting the half-maximal activation voltage ($V_{1/2}$) of the channel to more positive potentials (Figure 6B). C6 inhibition of mHv1 was dose-dependent, showing an

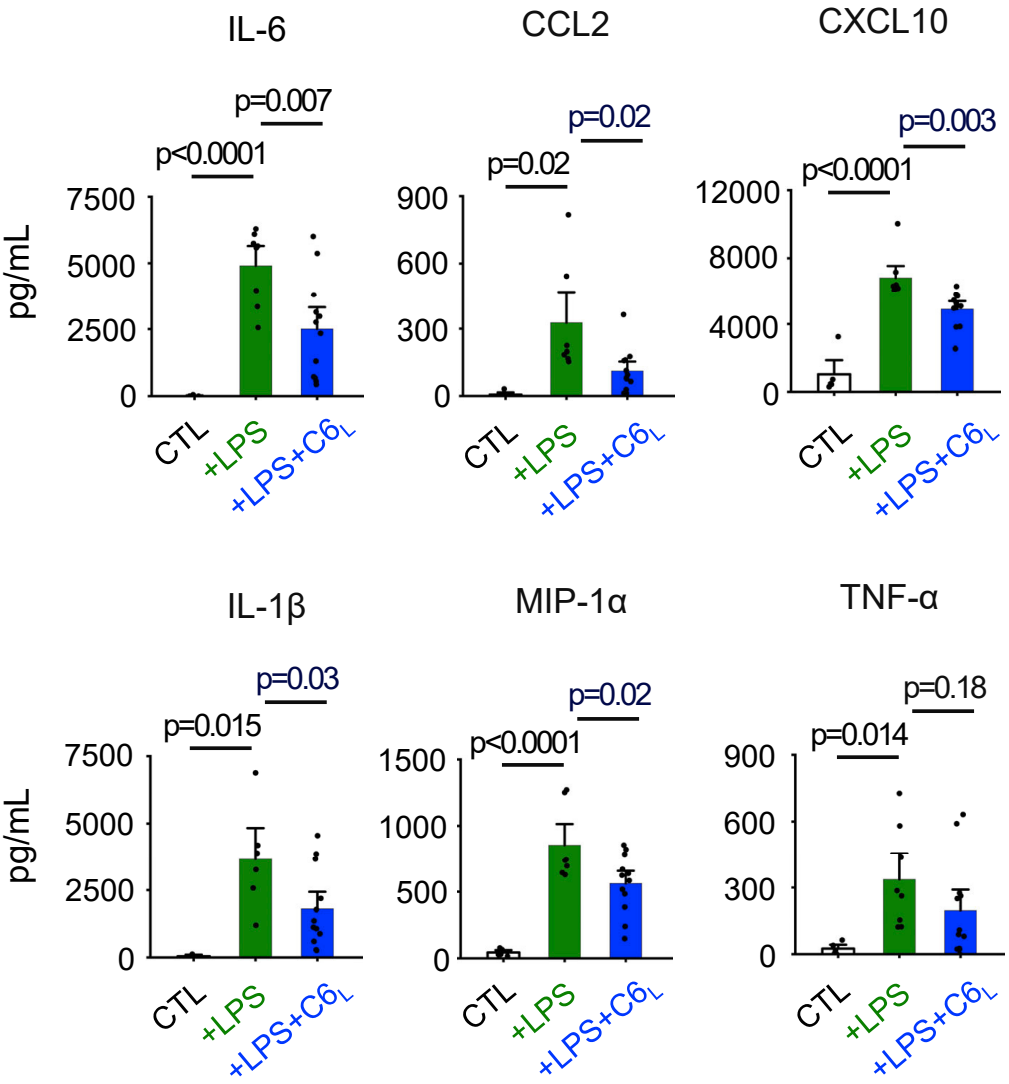

Figure 3. Effects of C6 on BAL fluid cytokine concentrations

Cytokine concentrations were quantified in BAL fluid using ELISA as described in STAR Methods. C6 (4 mg/kg) treatment decreased IL-6, CCL2, CXCL10, IL-1β, and MIP-1α concentrations, but not TNF-α, compared to groups receiving LPS. Control groups received injections of PBS. Values are mean ± SEM; n = 6-8 mice.

inhibitory constant K_i of 4.1 ± 0.3 nM and a Hill coefficient of 1.3 ± 0.1 at 0 mV as determined by fitting the dose-response curve to a Hill relationship (Figure 6C and STAR Methods). Thus, C6 was observed to be 3-fold less potent on mHv1 than on hHv1 (K_i = 1.5 nM at 0 mV).[11] This similar potency was expected given that the residues that bind C6 are homologous in the two channels (Figures S1A and S1C). Rationalizing why both low and high doses of C6 administered to the mice had significant effects on the LPS-treated mice (Figures 1 and 2), C6 at 20 nM decreased mHv1 currents by ~82%, shifting $V_{1/2}$ of the channel ~24 mV (Figures 6A and 6B), and 2 μM C6 decreased the currents ~95% (Figure 6C), shifting $V_{1/2}$ by ~35 mV.

C6 activity on lipopolysaccharide-treated human neutrophils

To support the relevance of these mouse studies to human ALI, it was important to confirm that C6 inhibited the release of ROS and elastase from human neutrophils resulting from stimulation by LPS. Indeed, in response to LPS (10 μM), freshly isolated human neutrophils showed a steady rise in ROS release using an Amplex Red assay to assess the extracellular ROS production (STAR Methods) that was inhibited by 1 μM C6 (Figure 7A), reducing release at 60 min by ~63% (Figure 7B). ROS also accumulates inside neutrophils

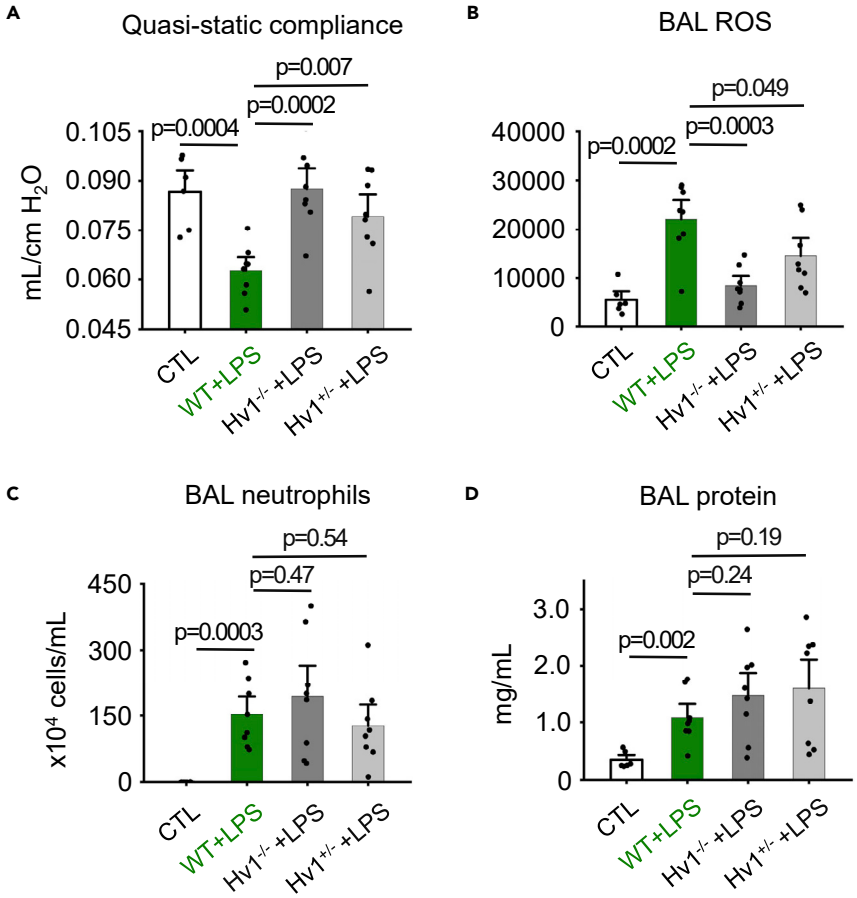

Figure 4. Hv1 deficiency protects mice against ALI

Experiments were conducted using WT, $Hv1^{-/-}$ and $Hv1^{+/-}$ mice (age- and gender-matched, n = 6-8). Basic pulmonary parameters of mice were measured 48 h post LPS induction as described in STAR Methods. Control groups received injections of PBS. Values are mean ± SEM.

(A) Quasi-static lung compliance measurements for WT, $Hv1^{-/-}$, and $Hv1^{+/-}$ mice subjected to LPS-induced ALI.

(B) ROS production from neutrophils from BALs of WT, $Hv1^{-/-}$, and $Hv1^{+/-}$ mice subjected to LPS-induced ALI.

(C) BAL neutrophils count for WT, $Hv1^{-/-}$, and $Hv1^{+/-}$ mice subjected to LPS-induced ALI.

(D) BAL fluid total protein measurements for WT, $Hv1^{-/-}$, and $Hv1^{+/-}$ mice subjected to LPS-induced ALI.

upon activation where it contributes to microbial killing during phagocytosis and modifies cell-signaling proteins that mediate processes such as inflammation.[18] Using a DCFDA-based assay to assess intracellular ROS in human neutrophils (STAR Methods), we observed that LPS increased ROS production ~3.1-fold and that C6 (1 μM) reduced the increase by ~57%, employing diphenyleneiodonium chloride (DPI) blockade to demonstrate that the signal was not due to confounding background or secondary effects (Figure 7C).[19,20]

Elastase is a serine protease stored in azurophilic granules of neutrophils and a well-established marker of neutrophil activation.[21] In addition to its function as a powerful host defense mechanism, neutrophil elastase is a destructive enzyme that disrupts the lung permeability barrier thereby contributing to the development of ALI.[21] We studied the release of elastase from human neutrophils using an activity assay (STAR Methods), observing that LPS increased release ~1.6-fold, and that the increase was reduced by ~77% by 1 μM C6 (Figure 7D).

DISCUSSION

Hv1 is a viable target to suppress acute lung injury

Despite the development of innovative therapies and intensive supportive care, ALI induced by bacteria and other microbes remains an unresolved challenge.[2,22] This has been highlighted by the COVID-19

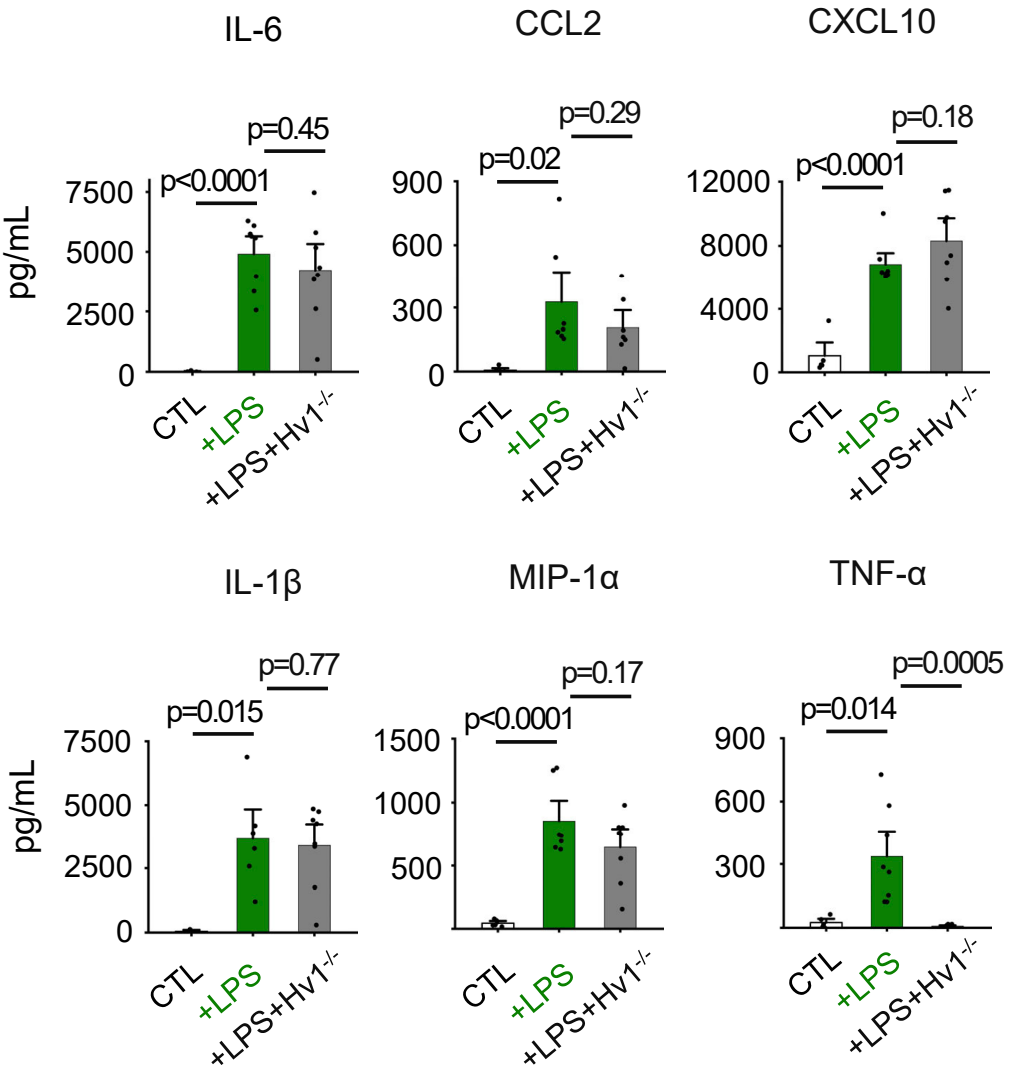

Figure 5. Effects of Hv1$^{-/-}$ on BAL fluid cytokine concentrations

Cytokine concentrations were quantified in BAL fluid using ELISA as described in STAR Methods. Hv1$^{-/-}$ only significantly decreased TNF-α concentration, compared to groups receiving LPS. Control groups received injections of PBS. Values are mean ± SEM; n = 6-8 mice.

pandemic; while SARS-CoV-2 infection can be mild, death frequently results from pneumonia that progress to ALI and ARDS due to the release of inflammatory mediators from neutrophils.[22] Here we demonstrate that Hv1 is a viable target to suppress inflammatory ALI showing that C6, a peptide designed to specifically block the channel, protects mice from *i.t.* LPS-induced ALI (Figure 1) and suppresses ROS and elastase release from human neutrophils in response to LPS (Figure 7). Supporting our hypothesis that decreasing Hv1 activity opposes the deleterious effects of LPS-induced ALI, protection was also induced by genetic manipulation in mice to decrease or ablate Hv1 expression (Figure 4). Thus, we observed lower ROS release by neutrophils from Hv1$^{-/-}$ mice treated with LPS *i.t.* compared to WT mice, consistent with two groups who reported decreased ROS release from neutrophils isolated from Hv1$^{-/-}$ mice challenged *in vitro* with PMA compared to WT mice, one using the knockout strain we use, donated to us by Wu[9,16] and the other using a strain generated differently.[10] A fourth group observed the latter strain to increase ROS release from isolated neutrophils in response to PMA.[23] It is important to note that we employ LPS to recapitulate the downstream ALI effects of infection rather than live microorganisms. This is likely to explain why we see only salutary effects of C6 inhibition of the neutrophil inflammatory response, whereas with Hv1$^{-/-}$ mice administered *Staphylococcus aureus* intraperitoneally showed higher bacterial counts in the

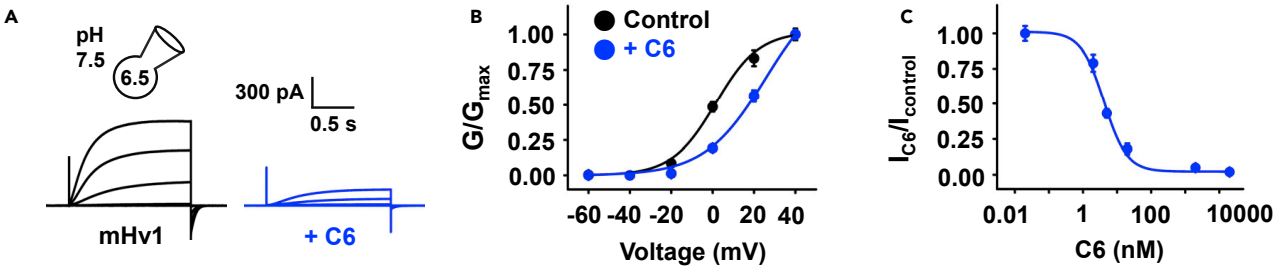

Figure 6. C6 peptide inhibits mHv1 potently

mHv1 channels were expressed in HEK293T cells and studied by whole-cell patch clamp to assess block parameters using a holding voltage of −60 mV, 1.5-s test pulses, and a 10-s interpulse interval, with pH_i = 6.5 and pH_o = 7.5. Values are mean ± SEM; n = 5 cells for each condition.

(A) Representative proton current traces for mHv1 channels before (Left), and in the presence of 20 nM C6 (Right) with steps of 20 mV from −60 to +40 mV. The peak current measured at the end of the depolarization pulse was used to determine the extent of block.

(B) Conductance-voltage relationships (G-V) for mHv1 in the absence or presence of 20 nM C6 (blue). Curves are fitting to the Boltzmann equation (STAR Methods).

(C) Dose-response relationships for C6 inhibition of mHv1. The inhibition constant K_i of C6 for mHv1 channels was estimated from the fit to Hill equation (STAR Methods) and was 4.1 ± 0.3 nM with a Hill coefficient of 1.3 ± 0.1.

peritoneal lavage fluid than WT mice,[9] and severe lung inflammation followed intranasal administration of *Candida albicans* to $Hv1^{-/-}$ mice,[23] consistent with neutrophils from the knockout mice offered diminished innate immune suppression of infective cell growth.

C6 treatment decreased the rise in the levels of CCL2, CXCL10, MIP-1α, and IL-1β in BAL fluid in the LPS-treated mice and this may also contribute to its protective effects (Figure 3). Thus, CCL2 has been shown to contribute to neutrophil recruitment to the lungs in ALI[24] and elevated CCL2 levels are observed in BAL fluid samples from patients with ARDS.[15] CXCL10 and MIP-1α are also proinflammatory cytokines that mediate leukocyte trafficking.[25,26] Direct neutralization of CXCL10 by antibody administration has been shown to ameliorate the severity of LPS-induced ARDS in rats by reducing pulmonary edema, limiting immune cell influx into the lungs, and inhibiting the release of other inflammatory cytokines.[27] IL-1β is also a neutrophil activator[28] that is linked to increased vascular permeability in the lungs of patients with ALI.[29,30] Unexpectedly, we found that $Hv1^{-/-}$ only reduced the rise in the level of TNF-α in BAL, whereas the levels of IL-6, CCL2, CXCL10, IL-1β, and MIP-1α were not decreased significantly (Figure 5). The observation that CCL2, the cytokine that regulates the migration of neutrophils, was not significantly decreased in $Hv1^{-/-}$ mice after LPS induction may explain why knockout mice did not show reduced neutrophil counts in BAL nor an improved lung injury score. The differences between the transient blockade of Hv1 channels and their constitutive, global absence indicates that there are compensatory changes in the deletion of the Hv1 gene and may reflect uneven tissue distribution of C6, as we consider further later in discussion.

C6 also reduced LPS-induced increases in total protein and neutrophils in BAL fluid of WT mice (Figures 1E and 2A), whereas the Hv1 knockout did not. We suspect this reflects the timing of C6 administration, 5 h after the inflammatory stimulus in WT mice, allowing the channel to operate normally beforehand, or a compensatory change in the knockout animals lacking Hv1 constitutively. Future studies will assess the effect of C6 administered at other times after ALI induction.

Cellular target of C6 action in acute lung injury/acute respiratory distress syndrome

The healthy lung facilitates rapid gas transfer across distal alveolar-capillary units comprised of monolayers of endothelial and epithelial cells that restrict the passage of solutes and fluid but allow diffusion of carbon dioxide and oxygen.[2] Neutrophils are not present in the healthy alveoli.[2] During infection, alveolar epithelial cells, endothelial cells, and resident macrophages secrete cytokines, notably, IL-6, CCL2, CXCL10, MIP-1α, and IL-1β that recruit and activate circulating neutrophils to migrate into the alveoli, damaging the alveolar-capillary barrier[2] by the release of ROS and proteases that damage endothelial and epithelial cells, allowing the influx of fluid into the air spaces causing hypoxemia.[31] Thus, neutrophils are implicated as central to the initiation and propagation of ALI/ARDS,[6] a conclusion supported by the observation that the concentration of neutrophils in BAL fluid correlates with severity of the disease and outcome.[5]

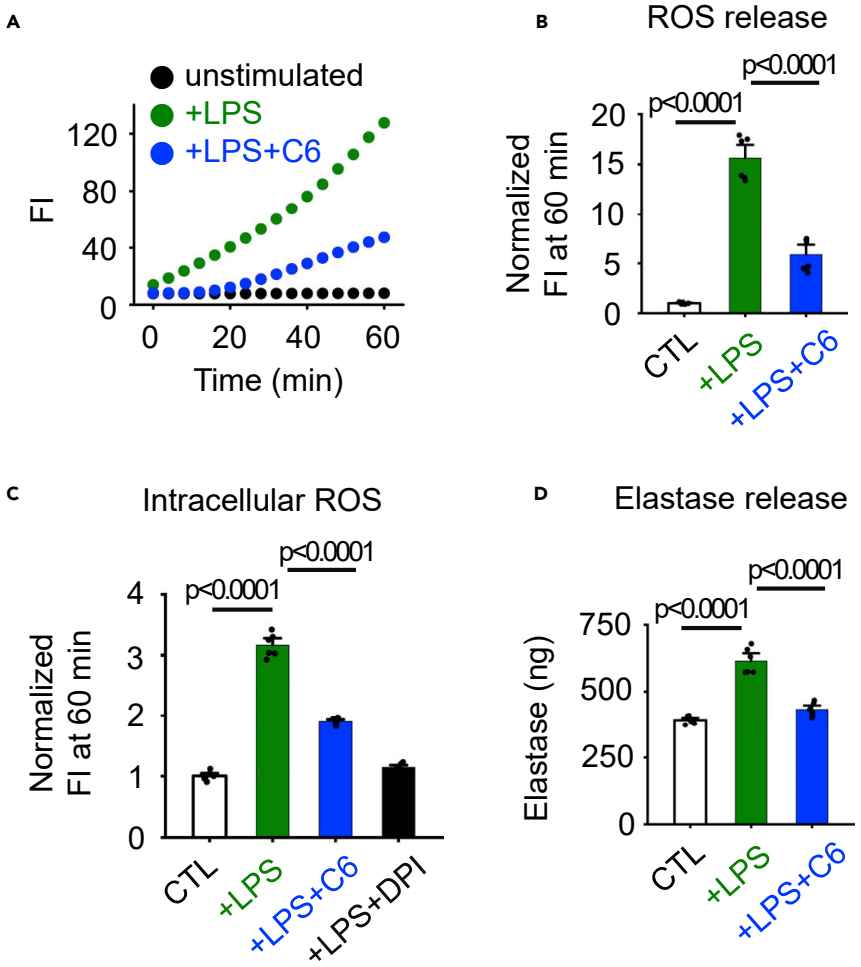

Figure 7. C6 suppresses LPS-induced ROS production and elastase release from human neutrophils

Human neutrophils were isolated from the peripheral blood of healthy volunteers and studied using a microplate fluorometer (STAR Methods). Values are mean ± SEM; n = 6 for each condition.

(A) Effect of LPS (10 μM) alone or in combination with C6 peptide (1 μM) on ROS release by human neutrophils (2×10^5 cells). ROS was measured using Amplex Red, a fluorescent probe for extracellular H_2O_2.

(B) ROS release 60 min after LPS stimulation. Values are normalized to mean ROS release by neutrophils without LPS stimulation (CTL).

(C) Effect of LPS (10 μM) alone or in combination with C6 peptide (1 μM) on intracellular ROS production by human neutrophils (2×10^5 cells), 60 min after LPS stimulation. ROS was measured using the cell-permeable fluorescent probe DCFDA. Diphenyleneiodonium chloride (DPI), an inhibitor of NADPH oxidase, was used to show the signal was specific and not due to background or secondary effects. Values are normalized to mean ROS release by neutrophils without LPS stimulation (CTL).

(D) Effect of LPS (10 μM) alone or in combination with C6 peptide (1 μM) on total elastase release by human neutrophils (1×10^6 cells) measured fluorometrically using neutrophil elastase activity assay. Control is elastase release by neutrophils without LPS stimulation.

Consistent with these reports, we observed that neutrophils were negligible in healthy mouse lungs but accounted for ~93% of the cells recovered in the BAL fluid of LPS-treated mice (Figure 2B). C6 treatment significantly reduced the number of neutrophils and ROS in the BAL fluid of the LPS-treated mice (Figure 2A), and we suspect these changes are central to the protective effects of the C6 peptide. Although neutrophils are an important cellular target of C6 action in the LPS-treated mice, as the major source of ROS production in ALI/ARDS lungs,[32] Hv1 channels are also expressed on alveolar epithelial cells and macrophages[13] that produce many of the cytokines we study here. It seems likely that some of the salutary effects of C6 accrue from its action on Hv1 in these other cell types, notably to suppress cytokine secretion and, thereby, neutrophil migration. However, in our mice the large majority of cells in BAL fluid following

LPS stimulation are neutrophils (>90%) and, therefore, we do not believe that macrophages are major contributors to the observed injury.

We observed that the high dose of C6 (12 mg/kg) offered better protection of lung compliance than the low dose (4 mg/kg), whereas the high dose did not further improve the inflammation-associated parameters of BAL protein concentration, neutrophil number, and ROS level, or the lung injury score. We suspect this reflects the direct role of Hv1 in neutrophils on some aspects of inflammatory damage and that the low C6 dose achieves levels that would fully block the channel in some compartments where it is estimated to reach ~1 μM (STAR Methods), 240-fold higher than the K_i for mHv1 (Figure 6). In contrast, lung compliance is a measure of function and an endpoint reflective of the complex interplay of multiple physiological processes within the inflammatory environment, and thus may not show as direct a correlation with changes in Hv1 activity, especially if the channel has a major or secondary role in a location where the peptide has more limited access. For example, both the central and peripheral nervous systems control respiration, and if only 0.1% of C6 crosses the blood-brain barrier after i.v.[33,34] higher dose would increase CNS levels from 1 nM to 3 nM to produce greater block of mHv1. Finally, we study effects 48 h after LPS induction, and earlier measurements might reveal differences due to the kinetics of action of low and high doses of C6.

Molecular basis of C6 action

A central protective effect of C6 inhibition of Hv1 can be attributed to its suppression of ROS production by neutrophils. Neutrophils produce ROS through activation of nicotinamide adenine dinucleotide phosphate oxidase 2 (NOX2).[4] NOX2 transfers electrons across the membrane, resulting in membrane depolarization and cytoplasmic acidification that suppresses further ROS production.[35] C6 blocks H^+ efflux through Hv1 that is required to maintain physiological intracellular pH and membrane potential[8,36] thereby subduing the activity of NOX2 to suppress the release of ROS.[12] ROS serves as an important activating signal for neutrophils migration and protease release.[37] This could explain the dampened neutrophils influx (Figure 2A) and elastase release (Figure 7D) we observe in this study.

Hv1 in both mice and humans is comprised of two identical subunits of ~270 residues, each with four transmembrane spans (TMs) that resemble the voltage sensor domains (VSD) in other voltage-gated ion channels (VGICs) (Figure S1A).[38,39] In Hv1 channels, there are two H^+-conduction pathways, one in each subunit[40] whereas other VGICs have four VSDs each with two additional TMs that fold together to form one, central ion conduction pore in each channel.

The absence of specific, high-affinity blockers of Hv1 channels motivated our design of C6 peptide for the human variant to study the roles of the channel in physiology and to serve as a drug lead,[8] as we consider in the current work. Two C6 peptides bind to each hHv1 channel with positive cooperativity, one on the external VSD residues linking the third and fourth TMs (S3-S4 loop) of each subunit. C6 binding is more avid at hyperpolarized voltages, like the resting membrane potential of neutrophils (~−60 mV), when the Hv1 sensors are in the "down" conformation; binding therefore favors the channel closed state yielding an effective $K_i \sim 1.5$ nM at 0 mV.[8,11] Here, we study mouse Hv1 observing the C6 block to be like that for the human variant, but 3-fold less effective ($K_i \sim 4.1$ nM at 0 mV), presumably a reflection of the primary sequences of their S3-S4 loops where C6 binds that differ at only three residues and are 78% identical (Figure S1C). Supporting a high degree of discrimination, 1 μM C6 did not inhibit the mammalian K^+, Na^+, and Ca^{2+} channels we tested nor Hv1 from the sea squirt *Ciona intestinalis* despite its homology to mHv1 and hHv1.[8]

C6 has protective potential against human acute lung injury/acute respiratory distress syndrome

We show here that C6 protects against lung tissue damage and the release of inflammatory mediators in a murine model for infectious ALI (Figures 1, 2, and 3) and suppresses the LPS-induced release of ROS and elastase by human neutrophils (Figure 7). Among important questions that attend the consideration of C6 as a therapeutic agent is, first, the utility of peptides as drugs. To-date, more than 40 peptides have been approved as drugs in humans, six that are venom-derived.[41] Specifically supporting the potential use of C6 as a medication, the 41 residue peptide is stable in solution for many months without diminished activity, longevity we attribute to six cysteines that form three intramolecular disulfide bonds and maintain a 3D scaffold like that present in natural inhibitor cystine knot (ICK) toxins (Figures S1B and S1D).[8]

Another important question that attends the consideration of C6 as a drug is if Hv1 suppression causes major side effects. We found that *i.v.* administration of C6 was well tolerated by WT healthy mice and did not change baseline lung compliance (Figure S3A) or baseline BAL fluid levels of neutrophils and ROS (Figures S3C and S3D) nor did it produce overt signs of deleterious off-target impacts. Interestingly, C6 did decrease basal levels of BAL fluid protein (Figure S3B) and a similar decrease was observed in $Hv1^{-/-}$ mice compared to WT mice (Figure S4B), perhaps due to basal Hv1 function in epithelial cells. While the BAL fluid protein level in healthy mice is low (~0.35 mg/mL), it merits further study to assess if the decrease caused by C6 inhibition of Hv1, or deletion of the channel, is biologically relevant. Work by others with $Hv1^{-/-}$ mice supports the notion that channel inhibition can be tolerated since the animals did not manifest obvious phenotypic disorders or malformations,[9,42] retained normal bacterial clearance in an infection model of sepsis[9] and showed less damage when subjected to middle cerebral artery occlusion-induced ischemic stroke.[16]

One disadvantage of unmodified peptides as drugs is their short half-life, generally due to fast renal clearance.[43] Thus, venom-derived peptides similar in size to C6 have a half-life of ~1 h *in vivo*.[33,44] However, the maturation of peptide therapeutics has provided strategies to prolong their half-life including conjugation to high molecular weight polyethyleneglycol (PEG),[45] fusion into the complementary-determining regions of antibodies,[46] and modifications that inhibit protease degradation such as the protection of the termini, unnatural amino acid substitutions, and cyclization.[43] An advance specific to C6 that we recently achieved is an engineered form that is significantly more potent *in vitro* because it is bivalent ($C6_2$) and binds to both of its sites on Hv1 simultaneously.[11] We plan to study the pharmacokinetics of C6 and $C6_2$ to inform the consideration of the size and timing of doses and if modifications are required for therapeutic efficacy.

Regulation of intracellular pH is essential to health and disease.[47] Since its identification, hHv1 has been implicated in many biological processes including white blood cell immune responses,[9,10] sperm capacitation,[48] cancer cell proliferation,[49] and tissue damage after ischemic stroke.[16] The demonstration that C6 suppresses LPS-induced ALI in mice, and the specific targeting of Hv1 by C6 without apparent deleterious side effects, suggests the channel has a central role in ALI/ARDS pathogenesis, that Hv1 is a druggable target, and that C6 and its derivatives may find utility in this life-threatening disease and other acute and chronic inflammatory disorders mediated by the innate immune system.

Limitations of the study

The study shows that *i.v.* injection of C6 peptide protects mice from ALI induced by intratracheal administration of bacterial LPS. Although C6 reduced neutrophil influx and suppressed the release of ROS, proteases, and proinflammatory cytokines in the lungs, it is important to note that we employed LPS to recapitulate the downstream ALI effects of infection rather than live microorganisms. The efficacy of C6 in suppressing ALI induced by live bacteria and fungus remains to be explored in future work.

STAR★METHODS

Detailed methods are provided in the online version of this paper and include the following:

- KEY RESOURCES TABLE
- RESOURCE AVAILABILITY
  - Lead contact
  - Materials availability
  - Data and code availability
- EXPERIMENTAL MODEL AND SUBJECT DETAILS
  - Cell lines
  - Animals
- METHOD DETAILS
  - Molecular biology
  - C6 peptide synthesis and purification
  - Whole-cell patch-clamp
  - LPS-induced lung injury and C6 peptide administration
  - Quasi-static lung compliance measurements
  - Bronchoalveolar lavage (BAL) fluid collection, lung histology, protein and ROS level determination, and neutrophil and total cells counts

- Cytokine measurements by ELISA
- Human peripheral blood neutrophils purification
- Neutrophil ROS measurement
- Neutrophil elastase measurement

● QUANTIFICATION AND STATISTICAL ANALYSIS

SUPPLEMENTAL INFORMATION

Supplemental information can be found online at https://doi.org/10.1016/j.isci.2022.105901.

ACKNOWLEDGMENTS

We are grateful for grant support from the NIH [GM111716 to S.A.N.G., HL159711 to S.A.N.G. and R.Z., and HL146821 to A.S.; the US-Israel Binational Science Foundation (BSF 2017243) to S.A.N.G.; National Center for Research Resources and the National Center for Advancing Translational Sciences, NIH UL1 TR001414 to R.Z. We appreciate the generosity of Dr. Long-jun Wu who provided the $Hv1^{-/-}$ mouse strain.

AUTHOR CONTRIBUTIONS

R.Z., B.L., A.S., and S.A.N.G. designed research; R.Z. and B.L. performed research; R.Z., B.L., A.S., and S.A.N.G. wrote the article.

DECLARATION OF INTERESTS

Based in part on this work, patents WO/2018/126,111 (HV1 MODULATORS AND USES) and WO/2022/251,637 (COMPOSITIONS AND METHODS FOR INHIBITING AN INFLAMMATORY RESPONSE AND TREATING INFLAMMATORY DISEASES) have been published.

Received: February 27, 2022
Revised: December 6, 2022
Accepted: December 27, 2022
Published: January 20, 2023

REFERENCES

1. Diaz, J.V., Brower, R., Calfee, C.S., and Matthay, M.A. (2010). Therapeutic strategies for severe acute lung injury. Crit. Care Med. *38*, 1644–1650. https://doi.org/10.1097/CCM.0b013e3181e795ee.

2. Matthay, M.A., Zemans, R.L., Zimmerman, G.A., Arabi, Y.M., Beitler, J.R., Mercat, A., Herridge, M., Randolph, A.G., and Calfee, C.S. (2019). Acute respiratory distress syndrome. Nat. Rev. Dis. Primers *5*, 18. https://doi.org/10.1038/s41572-019-0069-0.

3. Rubenfeld, G.D., Caldwell, E., Peabody, E., Weaver, J., Martin, D.P., Neff, M., Stern, E.J., and Hudson, L.D. (2005). Incidence and outcomes of acute lung injury. N. Engl. J. Med. *353*, 1685–1693. https://doi.org/10.1056/NEJMoa050333.

4. Winterbourn, C.C., Kettle, A.J., and Hampton, M.B. (2016). Reactive oxygen species and neutrophil function. Annu. Rev. Biochem. *85*, 765–792. https://doi.org/10.1146/annurev-biochem-060815-014442.

5. Steinberg, K.P., Milberg, J.A., Martin, T.R., Maunder, R.J., Cockrill, B.A., and Hudson, L.D. (1994). Evolution of bronchoalveolar cell populations in the adult respiratory distress syndrome. Am. J. Respir. Crit. Care Med. *150*, 113–122. https://doi.org/10.1164/ajrccm.150.1.8025736.

6. Grommes, J., and Soehnlein, O. (2011). Contribution of neutrophils to acute lung injury. Mol. Med. *17*, 293–307. https://doi.org/10.2119/molmed.2010.00138.

7. DeCoursey, T.E. (2013). Voltage-gated proton channels: molecular biology, physiology, and pathophysiology of the H(V) family. Physiol. Rev. *93*, 599–652. https://doi.org/10.1152/physrev.00011.2012.

8. Zhao, R., Kennedy, K., De Blas, G.A., Orta, G., Pavarotti, M.A., Arias, R.J., de la Vega-Beltrán, J.L., Li, Q., Dai, H., Perozo, E., et al. (2018). Role of human Hv1 channels in sperm capacitation and white blood cell respiratory burst established by a designed peptide inhibitor. Proc. Natl. Acad. Sci. USA *115*, E11847–E11856. https://doi.org/10.1073/pnas.1816189115.

9. Ramsey, I.S., Ruchti, E., Kaczmarek, J.S., and Clapham, D.E. (2009). Hv1 proton channels are required for high-level NADPH oxidase-dependent superoxide production during the phagocyte respiratory burst. Proc. Natl. Acad. Sci. USA *106*, 7642–7647. https://doi.org/10.1073/pnas.0902761106.

10. El Chemaly, A., Okochi, Y., Sasaki, M., Arnaudeau, S., Okamura, Y., and Demaurex, N. (2010). VSOP/Hv1 proton channels sustain calcium entry, neutrophil migration, and superoxide production by limiting cell depolarization and acidification. J. Exp. Med. *207*, 129–139. https://doi.org/10.1084/jem.20091837.

11. Zhao, R., Shen, R., Dai, H., Perozo, E., and Goldstein, S.A.N. (2022). Molecular determinants of inhibition of the human proton channel hHv1 by the designer peptide C6 and a bivalent derivative. Proc. Natl. Acad. Sci. USA *119*. e2120750119. https://doi.org/10.1073/pnas.2120750119.

12. Zhao, R., Dai, H., Arias, R.J., De Blas, G.A., Orta, G., Pavarotti, M.A., Shen, R., Perozo, E., Mayorga, L.S., Darszon, A., and Goldstein, S.A.N. (2021). Direct activation of the proton channel by albumin leads to human sperm capacitation and sustained release of inflammatory mediators by neutrophils. Nat. Commun. *12*, 3855. https://doi.org/10.1038/s41467-021-24145-1.

13. Seredenina, T., Demaurex, N., and Krause, K.H. (2015). Voltage-gated proton channels as novel drug targets: from NADPH oxidase regulation to sperm biology. Antioxid. Redox Signal. *23*, 490–513. https://doi.org/10.1089/ars.2013.5806.

14. Domscheit, H., Hegeman, M.A., Carvalho, N., and Spieth, P.M. (2020). Molecular dynamics of lipopolysaccharide-induced lung injury in rodents. Front. Physiol. *11*, 36. https://doi.org/10.3389/fphys.2020.00036.

15. Williams, A.E., José, R.J., Mercer, P.F., Brealey, D., Parekh, D., Thickett, D.R., O'Kane, C., McAuley, D.F., and Chambers, R.C. (2017). Evidence for chemokine synergy during neutrophil migration in ARDS. Thorax *72*, 66–73. https://doi.org/10.1136/thoraxjnl-2016-208597.

16. Wu, L.J., Wu, G., Akhavan Sharif, M.R., Baker, A., Jia, Y., Fahey, F.H., Luo, H.R., Feener, E.P., and Clapham, D.E. (2012). The voltage-gated proton channel Hv1 enhances brain damage from ischemic stroke. Nat. Neurosci. *15*, 565–573. https://doi.org/10.1038/nn.3059.

17. Beeton, C., Wulff, H., Barbaria, J., Clot-Faybesse, O., Pennington, M., Bernard, D., Cahalan, M.D., Chandy, K.G., and Béraud, E. (2001). Selective blockade of T lymphocyte K(+) channels ameliorates experimental autoimmune encephalomyelitis, a model for multiple sclerosis. Proc. Natl. Acad. Sci. USA *98*, 13942–13947. https://doi.org/10.1073/pnas.241497298.

18. Dahlgren, C., Karlsson, A., and Bylund, J. (2019). Intracellular neutrophil oxidants: from laboratory curiosity to clinical reality. J. Immunol. *202*, 3127–3134. https://doi.org/10.4049/jimmunol.1900235.

19. Tetz, L.M., Kamau, P.W., Cheng, A.A., Meeker, J.D., and Loch-Caruso, R. (2013). Troubleshooting the dichlorofluorescein assay to avoid artifacts in measurement of toxicant-stimulated cellular production of reactive oxidant species. J. Pharmacol. Toxicol. Methods *67*, 56–60. https://doi.org/10.1016/j.vascn.2013.01.195.

20. Zheng, Y., Niyonsaba, F., Ushio, H., Nagaoka, I., Ikeda, S., Okumura, K., and Ogawa, H. (2007). Cathelicidin LL-37 induces the generation of reactive oxygen species and release of human alpha-defensins from neutrophils. Br. J. Dermatol. *157*, 1124–1131. https://doi.org/10.1111/j.1365-2133.2007.08196.x.

21. Kawabata, K., Hagio, T., and Matsuoka, S. (2002). The role of neutrophil elastase in acute lung injury. Eur. J. Pharmacol. *451*, 1–10. https://doi.org/10.1016/s0014-2999(02)02182-9.

22. Li, L., Huang, Q., Wang, D.C., Ingbar, D.H., and Wang, X. (2020). Acute lung injury in patients with COVID-19 infection. Clin. Transl. Med. *10*, 20–27. https://doi.org/10.1002/ctm2.16.

23. Okochi, Y., Aratani, Y., Adissu, H.A., Miyawaki, N., Sasaki, M., Suzuki, K., and Okamura, Y. (2016). The voltage-gated proton channel Hv1/VSOP inhibits neutrophil granule release. J. Leukoc. Biol. *99*, 7–19. https://doi.org/10.1189/jlb.3HI0814-393R.

24. Zemans, R.L., and Matthay, M.A. (2017). What drives neutrophils to the alveoli in ARDS? Thorax *72*, 1–3. https://doi.org/10.1136/thoraxjnl-2016-209170.

25. Liu, M., Guo, S., Hibbert, J.M., Jain, V., Singh, N., Wilson, N.O., and Stiles, J.K. (2011). CXCL10/IP-10 in infectious diseases pathogenesis and potential therapeutic implications. Cytokine Growth Factor Rev. *22*, 121–130. https://doi.org/10.1016/j.cytogfr.2011.06.001.

26. Zeng, X., Moore, T.A., Newstead, M.W., Hernandez-Alcoceba, R., Tsai, W.C., and Standiford, T.J. (2003). Intrapulmonary expression of macrophage inflammatory protein 1alpha (CCL3) induces neutrophil and NK cell accumulation and stimulates innate immunity in murine bacterial pneumonia. Infect. Immun. *71*, 1306–1315. https://doi.org/10.1128/IAI.71.3.1306-1315.2003.

27. Lang, S., Li, L., Wang, X., Sun, J., Xue, X., Xiao, Y., Zhang, M., Ao, T., and Wang, J. (2017). CXCL10/IP-10 neutralization can ameliorate lipopolysaccharide-induced acute respiratory distress syndrome in rats. PLoS One *12*, e0169100. https://doi.org/10.1371/journal.pone.0169100.

28. Prince, L.R., Allen, L., Jones, E.C., Hellewell, P.G., Dower, S.K., Whyte, M.K.B., and Sabroe, I. (2004). The role of interleukin-1beta in direct and toll-like receptor 4-mediated neutrophil activation and survival. Am. J. Pathol. *165*, 1819–1826. https://doi.org/10.1016/s0002-9440(10)63437-2.

29. Ganter, M.T., Roux, J., Miyazawa, B., Howard, M., Frank, J.A., Su, G., Sheppard, D., Violette, S.M., Weinreb, P.H., Horan, G.S., et al. (2008). Interleukin-1beta causes acute lung injury via alphavbeta5 and alphavbeta6 integrin-dependent mechanisms. Circ. Res. *102*, 804–812. https://doi.org/10.1161/CIRCRESAHA.107.161067.

30. Pugin, J., Ricou, B., Steinberg, K.P., Suter, P.M., and Martin, T.R. (1996). Proinflammatory activity in bronchoalveolar lavage fluids from patients with ARDS, a prominent role for interleukin-1. Am. J. Respir. Crit. Care Med. *153*, 1850–1856. https://doi.org/10.1164/ajrccm.153.6.8665045.

31. Potey, P.M., Rossi, A.G., Lucas, C.D., and Dorward, D.A. (2019). Neutrophils in the initiation and resolution of acute pulmonary inflammation: understanding biological function and therapeutic potential. J. Pathol. *247*, 672–685. https://doi.org/10.1002/path.5221.

32. Chow, C.W., Herrera Abreu, M.T., Suzuki, T., and Downey, G.P. (2003). Oxidative stress and acute lung injury. Am. J. Respir. Cell Mol. Biol. *29*, 427–431. https://doi.org/10.1165/rcmb.F278.

33. Beeton, C., Pennington, M.W., Wulff, H., Singh, S., Nugent, D., Crossley, G., Khaytin, I., Calabresi, P.A., Chen, C.Y., Gutman, G.A., and Chandy, K.G. (2005). Targeting effector memory T cells with a selective peptide inhibitor of Kv1.3 channels for therapy of autoimmune diseases. Mol. Pharmacol. *67*, 1369–1381. https://doi.org/10.1124/mol.104.008193.

34. Ezan, E. (2013). Pharmacokinetic studies of protein drugs: past, present and future. Adv. Drug Deliv. Rev. *65*, 1065–1073. https://doi.org/10.1016/j.addr.2013.03.007.

35. DeCoursey, T.E., Morgan, D., and Cherny, V.V. (2003). The voltage dependence of NADPH oxidase reveals why phagocytes need proton channels. Nature *422*, 531–534. https://doi.org/10.1038/nature01523.

36. DeCoursey, T.E. (2004). During the respiratory burst, do phagocytes need proton channels or potassium channels, or both? Sci. STKE *2004*, pe21. https://doi.org/10.1126/stke.2332004pe21.

37. Görlach, A., Bertram, K., Hudecova, S., and Krizanova, O. (2015). Calcium and ROS: a mutual interplay. Redox Biol. *6*, 260–271. https://doi.org/10.1016/j.redox.2015.08.010.

38. Ramsey, I.S., Moran, M.M., Chong, J.A., and Clapham, D.E. (2006). A voltage-gated proton-selective channel lacking the pore domain. Nature *440*, 1213–1216. https://doi.org/10.1038/nature04700.

39. Sasaki, M., Takagi, M., and Okamura, Y. (2006). A voltage sensor-domain protein is a voltage-gated proton channel. Science *312*, 589–592. https://doi.org/10.1126/science.1122352.

40. Tombola, F., Ulbrich, M.H., and Isacoff, E.Y. (2008). The voltage-gated proton channel Hv1 has two pores, each controlled by one voltage sensor. Neuron *58*, 546–556. https://doi.org/10.1016/j.neuron.2008.03.026.

41. Wulff, H., Christophersen, P., Colussi, P., Chandy, K.G., and Yarov-Yarovoy, V. (2019). Antibodies and venom peptides: new modalities for ion channels. Nat. Rev. Drug Discov. *18*, 339–357. https://doi.org/10.1038/s41573-019-0013-8.

42. Okochi, Y., Sasaki, M., Iwasaki, H., and Okamura, Y. (2009). Voltage-gated proton channel is expressed on phagosomes. Biochem. Biophys. Res. Commun. *382*, 274–279. https://doi.org/10.1016/j.bbrc.2009.03.036.

43. Pennington, M.W., Czerwinski, A., and Norton, R.S. (2018). Peptide therapeutics from venom: current status and potential. Bioorg. Med. Chem. *26*, 2738–2758. https://doi.org/10.1016/j.bmc.2017.09.029.

44. Jin, L., Zhou, Q.T., Chan, H.K., Larson, I.C., Pennington, M.W., Morales, R.A.V., Boyd, B.J., Norton, R.S., and Nicolazzo, J.A. (2016). Pulmonary delivery of the Kv1.3-blocking peptide HsTX1[R14A] for the treatment of autoimmune diseases. J. Pharm. Sci. *105*, 650–656. https://doi.org/10.1016/j.xphs.2015.10.025.

45. Murray, J.K., Qian, Y.X., Liu, B., Elliott, R., Aral, J., Park, C., Zhang, X., Stenkilsson, M., Salyers, K., Rose, M., et al. (2015). Pharmaceutical optimization of peptide toxins for ion channel targets: potent, selective, and long-lived antagonists of Kv1.3. J. Med. Chem. *58*, 6784–6802. https://doi.org/10.1021/acs.jmedchem.5b00495.

46. Wang, R.E., Wang, Y., Zhang, Y., Gabrelow, C., Zhang, Y., Chi, V., Fu, Q., Luo, X., Wang, D., Joseph, S., et al. (2016). Rational design of a Kv1.3 channel-blocking antibody as a selective immunosuppressant. Proc. Natl. Acad. Sci. USA *113*, 11501–11506. https://doi.org/10.1073/pnas.1612803113.

47. Roos, A., and Boron, W.F. (1981). Intracellular pH. Physiol. Rev. *61*, 296–434. https://doi.org/10.1152/physrev.1981.61.2.296.

48. Lishko, P.V., Botchkina, I.L., Fedorenko, A., and Kirichok, Y. (2010). Acid extrusion from human spermatozoa is mediated by flagellar voltage-gated proton channel. Cell *140*, 327–337. https://doi.org/10.1016/j.cell.2009.12.053.

49. Wang, Y., Li, S.J., Pan, J., Che, Y., Yin, J., and Zhao, Q. (2011). Specific expression of the human voltage-gated proton channel Hv1 in highly metastatic breast cancer cells, promotes tumor progression and metastasis. Biochem. Biophys. Res. Commun. *412*, 353–359. https://doi.org/10.1016/j.bbrc.2011.07.102.

50. Musset, B., and Decoursey, T. (2012). Biophysical properties of the voltage gated proton channel H(V)1. Wiley interdisciplinary reviews. Wiley Interdiscip. Rev. Membr. Transp. Signal. *1*, 605–620. https://doi.org/10.1002/wmts.55.

51. Kalman, K., Pennington, M.W., Lanigan, M.D., Nguyen, A., Rauer, H., Mahnir, V., Paschetto, K., Kem, W.R., Grissmer, S., Gutman, G.A., et al. (1998). ShK-Dap22, a potent Kv1.3-specific immunosuppressive polypeptide. J. Biol. Chem. *273*, 32697–32707. https://doi.org/10.1074/jbc.273.49.32697.

52. Salazar, E., and Knowles, J.H. (1964). An analysis of pressure-volume characteristics of the lungs. J. Appl. Physiol. *19*, 97–104. https://doi.org/10.1152/jappl.1964.19.1.97.

53. Schwingshackl, A., Lopez, B., Teng, B., Luellen, C., Lesage, F., Belperio, J., Olcese, R., and Waters, C.M. (2017). Hyperoxia treatment of TREK-1/TREK-2/TRAAK-deficient mice is associated with a reduction in surfactant proteins. Am. J. Physiol. Lung Cell Mol. Physiol. *313*, L1030–L1046. https://doi.org/10.1152/ajplung.00121.2017.

STAR★METHODS

KEY RESOURCES TABLE

REAGENT or RESOURCE	SOURCE	IDENTIFIER
Chemicals, peptides, and recombinant proteins		
C6 Peptide	Zhao et al.[8]	https://doi.org/10.1073/pnas.1816189115 GenBank: AZI15804
Lipopolysaccharides	Cell Signaling	Cat# 41011S
DMSO	Sigma-Aldrich	Cat# D2650
PBS	Gibco	Cat# 10010023
Ficoll Paque Plus	GE Healthcare	Cat# GE17-1440-02
Dextran	Sigma-Aldrich	Cat# 31392
1x RBC Lysis Buffer	eBioscience	Cat# 00-4333-57
Critical commercial assays		
Bradford protein assay	Bio-Rad	Cat# 5000201
Diff-Quick stain	Fisher Sci	Cat# NC1796273
Cellular ROS assay	ThermoFisher	Cat# C400
DCFDA/H2DCFDA Cellular ROS Assay	Abcam	Cat# ab113851
Amplex™ red hydrogen peroxide/peroxidase assay	ThermoFisher	Cat# A22188
Neutrophil elastase activity assay	Abcam	Cat# ab204730
Mouse IL-6 ELISA	BD Biosci	Cat# 555240
Mouse CCL2 ELISA	BD Biosci	Cat# 555260
Mouse CXCL10 ELISA	R&D Systems	Cat# DY466
Mouse IL-1β ELISA	R&D Systems	Cat# DY401
Mouse MIP-1α ELISA	R&D Systems	Cat# DY450
Mouse TNF-α ELISA	BD Biosci	Cat# 560478
EasySep™ Mouse Neutrophil Enrichment Kit	STEMCELL Technologies	Cat # 19762
Experimental models: Cell lines		
Human Embryonic Kidney (HEK) 293T	ATTC	Cat# CRL-3216; RRID:CVCL_0063
Human Peripheral Blood Neutrophils	UCI: ICTS	N/A
Experimental models: Organisms/strains		
C57BL/6J mice	Jackson Laboratories	N/A
$Hv1^{-/-}$ mice	Ramsey et al.[9]	N/A
$Hv1^{+/-}$ mice	This study	N/A
Recombinant DNA		
mHv1-pMax	This study	GenBank: NM_001042489
Software and algorithms		
pClamp version 10	Molecular Devices	N/A
Origin version 8	Microcal	N/A
Prism version 8	GraphPad	N/A
SkanIt Software version 6.02 for Microplate Readers	ThermoFisher	N/A

RESOURCE AVAILABILITY

Lead contact

Further information and requests for resources and reagents should be directed to and will be fulfilled by the lead contact, Steve A.N. Goldstein (sgoldst2@uci.edu).

Materials availability

All plasmids and peptides generated in this study will be made available from the lead contact upon reasonable request.

Data and code availability

All data needed to evaluate the conclusions in the paper are present in the paper and the Supplementary Information. This paper does not report original code. Additional information is available from the lead contact upon request.

EXPERIMENTAL MODEL AND SUBJECT DETAILS

Cell lines

HEK293T cells were purchased from ATCC and maintained in Dulbecco's Modified Eagle Medium (DMEM) (ATCC) supplemented with 10% fetal bovine serum and 1% penicillin and streptomycin. Plasmids were transfected into cells using Lipofectamine 2000 (Life Technologies) according to the manufacturer's instructions and experiments preformed 24 h later.

Animals

All experiments were conducted using C57BL/6 wild-type (WT) mice, $Hv1^{+/-}$ mice and $Hv1^{-/-}$ mice aged 9–12 weeks. $Hv1^{-/-}$ mice generated using gene trap strategy[9] were a generous gift from Dr. Long-jun Wu. For experimental purposes, mice were age- and sex-matched (half males and half females). Approval for experiments in mice was obtained from the University of California, Los Angeles Animal Research Committee (ARC). All experiments were performed in accordance with institutional protocols, guidelines, and recommendations.

METHOD DETAILS

Molecular biology

Mouse Hv1 (NM_001042489) was constructed using gBlock gene fragments (Integrated DNA Technologies) and inserted into a laboratory dual purpose vector pMAX + using Gibson Assembly (New England BioLabs). The sequence mHv1 was confirmed by DNA sequencing.

C6 peptide synthesis and purification

C6 peptide (GenBank: AZI15804) was synthesized by CSBio. Peptide folding reactions were quenched by acidification and the peptides purified by HPLC, as before.[8] Peptides that were ~95% pure were lyophilized and stored at −20°C. Peptides were dissolved in solutions for *in vitro* or *in vivo* experiments before use.

Whole-cell patch-clamp

Proton currents passed by mHv1 were recorded in whole cell mode using an Axopatch 200B amplifier. Stimulation and data collection were done with a Digidata1322A and pCLAMP 10 software (Molecular Devices). Cells were perfused with an external bath solution comprised of 100 mM HEPES, 100 mM NaCl, 10 mM glucose at pH 7.5. Pipettes with resistances between 3 and 5 MΩ were filled with 100 mM Bis-Tris buffer, 100 mM NaCl, and 10 mM glucose at pH 6.5. Capacitance was subtracted online. Sampling frequency was 10 kHz with filtering at 1 kHz C6 block was monitored by evoking currents from a holding voltage of −60 mV with steps to 0 mV for 1.5 s with a 10 s interpulse interval. Current-voltage relationships were similarly evoked from a holding potential of −60 mV to test pulses from −60 mV to +40 mV for 1.5 s in 20 mV intervals every 10 s. Fractional unblocked current was assessed at the end of the test pulse. The conductance-voltage relationships were determined as described by De-Coursey in[50] and were fit to the Boltzmann equation, $G = G_{max}/[1 + \exp(-zF(V-V_{1/2})/RT)]$, where V is the test potential, $V_{1/2}$ is the voltage of half-maximal activation, z is the effective valence, T is the temperature, R is the gas constant, and F is the Faraday constant. Dose-response curves were determined by plotting the fractional unblocked current, $I_{C6}/I_{control}$, versus toxin concentration and fit with a Hill equation: $F_{un} = (1 + ([C6]/K_i)^h)^{-1})$, where F_{un} is the fraction of unblocked current at equilibrium, [C6] the effective C6 concentration, K_i the inhibition constant and h the Hill coefficient.

Mouse neutrophils were isolated from ~1 mL mouse peripheral blood using EasySep Mouse Neutrophil Enrichment Kit per the manual. Whole-cell patch clamp was used to record H^+ currents from neutrophils plated on poly-lysine coated coverslips. Pipettes (10–15 MΩ) were filled with 135 mM N-methyl-D-glucamine (NMDG), 5 mM ethylene glycol tetraacetic acid (EGTA), and 100 mM MES adjusted to pH 6.0

with methanesulfonic acid (CH_3SO_3H). Bath solution contains 130 mM NMDG, 1 mM EGTA and 100 mM HEPES, pH 7.5 with methanesulfonic acid.

LPS-induced lung injury and C6 peptide administration

Mice were anesthetized with brief inhalation of isofluorane (2–5%) anesthesia until they lost consciousness, then were suspended by their incisors on a 3.0 silk suture mounted on a 45°-angled stand. The tongue was gently extracted from the mouth and moved to the side using blunt forceps to visualize the vocal cords. Using fiberoptic guidance, a 20-gauge angiocatheter was passed through the vocal cords into the subglottic area, and 40 μL of LPS (10 mg/kg) or PBS control were injected with a micropipettor. We chose to deliver 10 mg/kg LPS for induction based on our pilot time- and dose-response studies. At 48 h, this LPS dose provided a clinically relevant model by producing moderate-severe acute lung injury, particularly, a significant decrease in lung compliance, in animals that could survive the challenge. This dose offered opportunity to model a meaningful therapeutic intervention. Mice were then placed back into their native cages and allowed to recover under a warming lamp until fully awake. No perianesthetic deaths were associated with this procedure. C6 stock solution were prepared in a mixture of DMSO and PBS (DMSO:PBS = 1:20). Two different concentrations of C6 were tested (C6 high dose = 12 mg/kg, C6 low dose = 4 mg/kg). This high injection dosing was used to study rats (intraperitoneal injection) and mice (*i.v.* injection) with the toxin peptide ShK, which is similar in size and composition to C6, producing a tissue concentration of ~3 μM,[17,51] 700-fold higher than the K_i of C6 for mHv1. Five hours after the LPS administration, the first dose of C6 (100 μL) was injected via the retro-orbital vein. At 24 h after LPS administration, a second dose of C6 (100 μL) was injected. Vehicle controls for C6 contained DMSO and PBS (DMSO:PBS = 1:20).

Quasi-static lung compliance measurements

After 48 h of LPS infection, a tracheostomy was performed using an 18-gauge steel catheter under general ketamine/xylazine anesthesia (intraperitoneal injection, 100 mg/kg ketamine, 12.5 mg/kg xylazine). Quasi-static lung compliance was measured using the Flexivent system (SCIREQ). Pressure–volume curves (P–V) were recorded, and each set of P–V curves was preceded by an inflation maneuver to total lung capacity to insure equal standard lung volumes for each experiment. Quasi-static lung compliance was calculated by fitting data derived from the P–V curves to the Salazar-Knowles equation.[52] Rectal temperatures were maintained in physiologic range using a heat lamp. All experiments were terminal.

Bronchoalveolar lavage (BAL) fluid collection, lung histology, protein and ROS level determination, and neutrophil and total cells counts

Following lung compliance measurements, BAL fluid was collected from all mice using a 1 mL syringe attached to the tracheostomy catheter. Two washouts were performed with 1 mL PBS/0.6 mM EDTA for BAL protein and cell count determination, and 1 mL PBS/0.5% BSA for cytokine assays. All samples were immediately placed on ice. Total BAL protein concentrations were measured using the Bradford assay (BioRad), and total BAL cell and neutrophils counts were performed using a Diff-Quick stain (Fisher Scientific). ROS production in BAL fluid cells was measured using Carboxy-H2DCFDA in a Cellular ROS Assay (ThermoFisher). Following BAL fluid collection, mice were euthanized via cardiac puncture and lungs were removed for histological examination. Briefly, the lungs were gently retrograde perfused via the right ventricle with 10 mL ice-cold PBS to remove red blood cells. Lung tissue was then removed *en bloc* and immediately perfused and fixed in 4% formalin. Paraffin embedded sections were cut into 4 μm thick tissues slices using a Microtome, and H&E-stained for histology. Two sets of slides were prepared and analyzed for each mouse. Lung injury scores were determined by an investigator blinded to the experimental conditions on H&E-stained lung sections as previously described,[53] using the following 3 criteria: (1) interstitial edema, (2) cellular infiltrate, and (3) parenchymal, peribronchial and perivascular hemorrhage. Each criterion was assigned a score between 0 and 3, with "0" representing no injury, "1" representing mild injury, "2" representing moderate injury, and "3" representing severe injury. Four randomly assigned high power fields per slide were scored under 20x magnification on a Motic AE20/21 inverted microscope, and scores were averaged for each criterion. Using the sum of these averages, a composite histological lung injury score was calculated for each experimental group.

Cytokine measurements by ELISA

Cytokine concentrations were quantified in BAL fluid after centrifugation at 8000 rpm for 5 min. Briefly, 100 μL of sample was loaded into 96-well species specific ELISA plates and analyzed in triplicates following the manufacturer's instructions. All samples were run in triplicates and values are displayed in pg/mL.

Human peripheral blood neutrophils purification

Human polymorphonuclear neutrophils were isolated from peripheral blood from healthy donors by Ficoll-Paque Plus (GE Healthcare) density-gradient centrifugation. Peripheral blood was obtained from Institute for Clinical and Translational Science of University of California Irvine and the protocol was approved by the Institutional Review Board of University of California Irvine. Donor population is composed of 50% female and 50% male with ages ranging from 23 to 62 years. Blood (20 mL) was mixed with 3% dextran in PBS (Sigma-Aldrich) for 20 min in a 50 mL conical tube. The top clear layer containing leukocytes was collected and underlaid with 10 mL of Ficoll-Paque Plus. The cell suspension was centrifuged at 500 g for 30 min at 20°C to separate mononuclear cells from neutrophils and the remaining red blood cells. The overlying plasma and monocyte layers were aspirated, and the neutrophils and red blood cells pellet was re-suspended in Red Blood Cells Lysis Buffer (eBioscience), incubated for 10 min to lyse red blood cells. 35 mL PBS was added to stop the lysis and the cell suspension was centrifuged at 300 g for 5 min at 4°C. Cell pellet was re-suspended in RPMI1640 (Gibco). An aliquot of neutrophils was mixed with Trypan blue (Gibco) and counted using a hemocytometer. Neutrophils isolated using this method were routinely found to be greater than 97% of the final cell preparation.

Neutrophil ROS measurement

Human neutrophils were isolated from peripheral blood and re-suspended in Hank's Balanced Salt Solution (HBSS) comprising 138 mM NaCl, 5.4 mM KCl, 0.34 mM Na_2HPO_4, 0.44 mM KH_2PO_4, 1.3 mM $CaCl_2$, 0.5 mM $MgCl_2$, 0.4 mM $MgSO_4$, 4.2 mM $NaHCO_3$, 5.5 mM glucose and 20 mM HEPES, pH 7.2, and dispensed into white 96-Well Immuno Plates (2×10^5 cells/well). Neutrophils ROS release was measured using Amplex Red Hydrogen Peroxide/Peroxidase Assay Kit (ThermoFisher) and the intracellular ROS was measured using DCFDA/H2DCFDA Cellular ROS Assay Kit (abcam). For the C6 group, neutrophils were pre-incubated with 1 μM C6 for 1 h before the assay. After incubation, neutrophils were stimulated with LPS (10 μM) and the fluorescence was measured immediately every 1 min for 60 min using Fluoroskan FL (ThermoFisher) equipped with internal software SkanIt 6.02.

Neutrophil elastase measurement

Human neutrophils were washed and re-suspended in HBSS. Elastase release from neutrophils was evaluated using Neutrophil Elastase Activity Assay Kit (abcam). Following the 1-h incubation without or with C6 (1 μM), neutrophils (1×10^6 cells) were subjected to stimulation using 10 μM LPS. Florescence was measured continually for 30 min using Fluoroskan FL. Elastase release (ng) was determined by comparing to the standard curve according to the kit manual.

QUANTIFICATION AND STATISTICAL ANALYSIS

Data were analyzed using the unpaired Student's *t* test (two-sided) and ANOVA test for multiple comparisons. All statistical analyses were performed using GraphPad Prism 6 software. $p \leq 0.05$ values were considered significant.